Asian Journal of Chemistry; Vol. 29, No. 11 (2017), 2379-2383

ASIAN JOURNAL OF CHEMISTRY

https://doi.org/10.14233/ajchem.2017.20674

Surface Characterization of Ni-Mg-Al and Co-Mg-Al Hydrotalcites by Inverse Gas Chromatography

ZHIYIN SUN[1,*], GUANGHUA XIA[2,3], WENYUAN TANG[1] and WENCHU WANG[4]

[1]Taizhou University, Taizhou 318000, P.R. China
[2]Zhejiang University of Technology, Hangzhou 310014, P.R. China
[3]Taizhou Pollution Control and Engineering Technology Center, Taizhou 318000, P.R.China
[4]TaiZhou Municipal Bureau of Forestry, Taizhou 318000, P.R. China

*Corresponding author: E-mail: 515198501@qq.com

Received: 27 March 2017; *Accepted*: 17 August 2017; *Published online*: 29 September 2017; AJC-18554

Carbonate pillared hydrotalcite-like compounds (Ni_xMg_{3-x}Al-LDHs and Co_xMg_{3-x}Al-LDHs) with different molar ratios were synthesized through co-precipitation and the samples were characterized by XRD, FTIR and inverse gas chromatography (IGC) techniques. The surface properties were compared and verified by computer simulation. The results indicated that with the increasing content of Ni^{2+} in Ni_xMg_{3-x}Al-LDHs, the surface adsorption free energy and dispersive component of the surface energy decreased, while the stability increased gradually, which was contrary to Co^{2+} in Co_xMg_{3-x}Al-LDHs. Besides, the surface free energy of Ni-Mg-Al hydrotalcites was smaller than Co-Mg-Al hydrotalicites when they were in the same molar ratio and the stability of the former was found to be stronger than the latter.

Keywords: Inverse gas chromatography, Hydrotalcites, Surface characterization.

INTRODUCTION

Layered double hydroxides (LDHs), also known as hydrotalcite-like compounds or anion clays, which are well known for their applications in the filed of catalysts, sorbents, composite additives, ion-exchangers, *etc*. [1,2]. Metal hydroxide with divalent and trivalent metal ions, with adjustable degeneration, can form hydrotalcite with catalytic activity by introducing with transition metal ions, such as Cu^{2+}, Ni^{2+}, Co^{2+}, *etc*. [3,4].

Recently, the study of Co^{2+} and Ni^{2+} hydrotalcites are generally focussed in catalysis and adsorption techniques. Zhao *et al*. [5] synthesized carbon nanotubes by using the calcined product of ternary magnesium nickel aluminum LDHs. The results showed that the catalytic properties is related to the content of nickel. Liu *et al*. [6] found that with the increase of cobalt content in LDHs, the catalytic activity of isopropanol increased and the catalytic product selectivity was also associated with the surface properties of hydrotalcite. Zhao [7] had researched benzaldehyde oxidation reaction by grafting Ni-Al-LDHs on carbon nanotubes as catalyst. The results showed that Ni-Al-LDHs had good catalytic performance and the main reason for the higher catalytic efficiency was the improvement of the catalyst dispersion. It's obvious that the surface properties of materials play a decisive role in catalysis and adsorption, which have important reference value for practical application. Considering the research on the surface properties of layered double hydroxides with catalytic activity is still very scarce, it's very meaningful to explore the surface properties of Ni-Mg-Al-LDHs and Co-Mg-Al-LDHs.

Inverse gas chromatography (IGC) is one of the most sensitive, reliable and convenient methods to study the surface properties [8]. This method was used to study the interaction between polymer and probe molecules and the compatibility between the polymers. In recent years, some researchers applied this technology in researching the surface properties of kaolin [9], montmorillonite [10] and other inorganic materials and modified materials.

By using this method, previous group [11,12] had studied the difference between the surface properties of Mg-Al-LDHs and its modified products, including Cu-Mg-Al-LDHs' surface properties. In this paper, we applied inverse gas chromatography (IGC) method to investigate the surface properties of Ni-Mg-Al-LDHs and Co-Mg-Al-LDHs. Simultaneously, the conclusion was validated by studying the stability and Jahn-Teller effect of the two systems with computer simulation [13].

EXPERIMENTAL

Sample preparation: Ni_xMg_{3-x}Al-LDHs (x = 0-3) were synthesized by a modified coprecipitation method [14]. An

aqueous solution (100 mL) named A was prepared with NaOH (0.2 mol) and Na_2CO_3 (0.025 mol), another aqueous solution (100 mL) named B was prepared with $Ni(NO_3)_2{\cdot}6H_2O$ (0.025 mol), $Mg(NO_3)_2{\cdot}6H_2O$ (0.05 mol) and $Al(NO_3)_3{\cdot}9H_2O$ (0.025 mol), after that both A and B were added dropwise to a three neck round bottom flask with vigorous stirring, maintaining the pH of 9 to 10, then keep stirring for 1h. After the reaction, the resulting precipitate was crystallized at 50 ºC for 18 h, and then centrifuged and washed with distilled water for several times and was finally dried *in vacuo* at 65 ºC for 12 h, giving the product $NiMg_2Al$-LDHs.

$NiMg_2Al$-LDHs, Ni_3Al-LDHs, Mg_3Al-LDHs, Co_3Al-LDHs, Co_2MgAl-LDHs and $CoMg_2Al$-LDHs were prepared by changing the mole ratio of Ni, Al and Mg according to the above described methods.

Inverse gas chromatography (IGC) analysis: A GC7890(II) gas chromatograph equipped with thermal conductivity detector, with high purity nitrogen (99.99 % pure) as the carrier gas at a flow rate of 50 mL/min, which was measured at the detector outlet with soap bubble flowmeter. Both the detector temperature and gasification chamber temperature were set at 453 K, and the column temperature was conditioned by heating at 403-433 K. Retention times were recorded on an N-2000 integrator. The probes used were *n*-pentane, *n*-hexane, *n*-heptane and *n*-octane, all reagents were obtained in the higher purity grade possibly and directly used as received.

X-ray diffraction (XRD) was carried out using a Shimadzu XRD-6000 diffractometer, with Cu-Kα radiation (λ = 0.1542 nm) at a scan speed of 5°/min. Bruker Vector 22 FT-IR spectra in the range 4000 - 400 cm^{-1} was used to analyze the structure of the sample (the mass ratio of sample to KBr was 1/100).

Preparation of chromatographic column: A stainless steel column with a length of 15 cm and an internal diameter of 0.2 cm. Clean it with acetone, leave to dry completely and then filled with the prepared LDHs materials respectively, after that all the columns were aged at 443 K under a constant nitrogen flow (30mL/min) for 1 h.

RESULTS AND DISCUSSION

Surface adsorption free energy: In this study, C_5-C_8 straight-chain alkanes as probe molecules, the intermolecular interaction force between molecules is neglected in the infinite dilution region. The relationship between adsorption free energy (ΔG^o) and retention volume (V_N) is described as follows [15,16]:

$$\Delta G° = -RT \ln V_N + C \quad (1)$$

$$V_N = (t_R - t_m)\cdot F_a \cdot \frac{T}{T_a}\cdot J \quad (2)$$

$$J = \frac{3}{2}\left(\frac{(p_i/p_o)^2 - 1}{(p_i/p_o)^3 - 1}\right) \quad (3)$$

where R is ideal gas constant, C is constant relative to the stationary phase, t_R and t_m are the retention time and dead times, T is the column temperature, F_a is the flow rate at the end of column at room temperature T_a, J is the James-Martin factor for the correction of gas compressibility, p_o is the outlet pressure and p_i is the inlet pressure.

The retention volume (V_N) was obtained by testing a series of probe molecules on the hydrotalcite-like compounds, and the corresponding surface free energy (ΔG^o) of adsorption were calculated and summarized in Table-1. As shown in Table-1, the surface adsorption free energy of all LDHs were below zero, indicating that the reaction of *n*-alkanes adsorbing on the solid surface could be carried out at room temperature spontaneously.

TABLE-1
$\Delta G°$ (KJ mol^{-1}) VALUES OF $Ni_xMg_{3-x}Al$-LDHs AND $Co_xMg_{3-x}Al$-LDHs (x = 0-3) AT 423 K

System	*n*-Pentane	*n*-Hexane	*n*-Heptane	*n*-Octane
Ni_3Al-LDHs	10.76	7.49	–	–
$MgNi_2Al$-LDHs	14.82	11.22	8.78	7.27
Mg_2NiAl-LDHs	16.12	12.96	11.11	8.53
Mg_3Al-LDHs	18.34	15.58	13.54	12.47
Mg_2CoAl-LDHs	10.97	7.80	5.35	5.35
$MgCo_2Al$-LDHs	16.56	13.88	12.12	10.64
Co_3Al-LDHs	16.61	14.29	–	–

According to the probe arrangements from the above list, *n*-alkane with more carbon atoms tends to have less surface adsorption free energy, this is due to the increasing of carbon atoms, the alkanes are getting more and more difficult to enter into the LDHs molecule structure or adsorb on it [12].

As we found in $Ni_xMg_{3-x}Al$-LDHs system, the surface free energy decreased with the increase of Ni^{2+} and this may be due to the introduction of Ni^{2+} that formed a more stable octahedron, which reduced the adsorption energy. While, as the content of Co^{2+} in Co/Mg/Al- LDHs systems increasing, a certain degree of distortion may occur in layer board structure, so the surface adsorption free energy increased.

By comparing the surface adsorption free energy of $Ni_xMg_{3-x}Al$-LDHs and $Co_xMg_{3-x}Al$-LDHs, it is found that the adsorption capacity of Co/Mg/Al-LDHs was larger than Ni/Mg/Al-LDHs if the x are equal, suggesting that LDHs with Co^{2+} possess more powerful surface activities.

Dispersive component of surface energy:

$$\gamma_s^d = \frac{1}{\gamma_{CH_2}}\cdot\left(\frac{\Delta G_{CH_2}}{2\cdot N\cdot \alpha_{CH_2}}\right)^2 \quad (4)$$

where N is Avogadro's number, γCH_2 is the surface energy of a hypothetical substance that contain only methylene groups and αCH_2 is the cross-sectional area of a methylene group (< 0.06 nm^2). Thus, at constant temperature, for a series of alkane probes, a plot of RTln V_N *versus* number of carbon atoms should give a straight line, and then obtained ΔG_{CH_2} from the linear slope.

As shown in Figs.1 and 2, RTln V_N of the material show a good linear relationship with the number of carbon number (the linear slope reflects the increment of the adsorption free energy), indicating that ΔG_{CH_2} is reliable and could be used to calculate γ_s^D at a high confidence level.

According to Dorris and Gray theory, with temperature 423 K, the surface energy dispersive component of solid surface could be calculated by eqn 4 and the results are listed in Table-2.

The γ_s^D can be used to assess the activity of solid surface [17]. Table-2 suggests that with the increasing of Ni^{2+} in

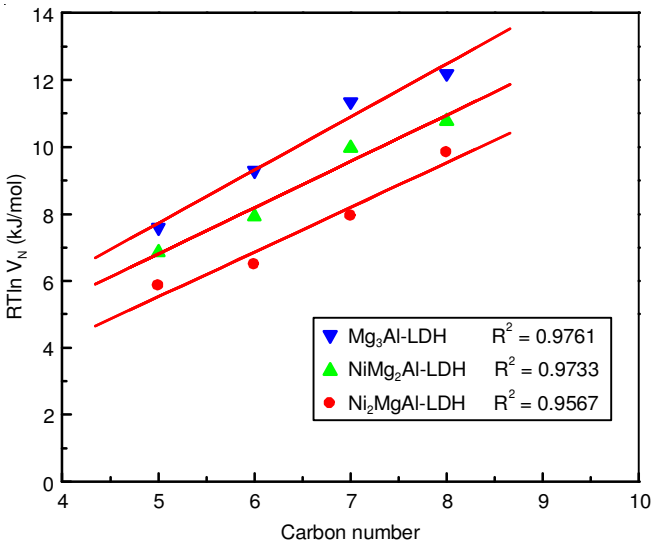

Fig. 1. Plot of RTln V_N values *versus* carbon number for $Ni_xMg_{3-x}Al$-LDHs (x = 0-2) to determine γ_s^d

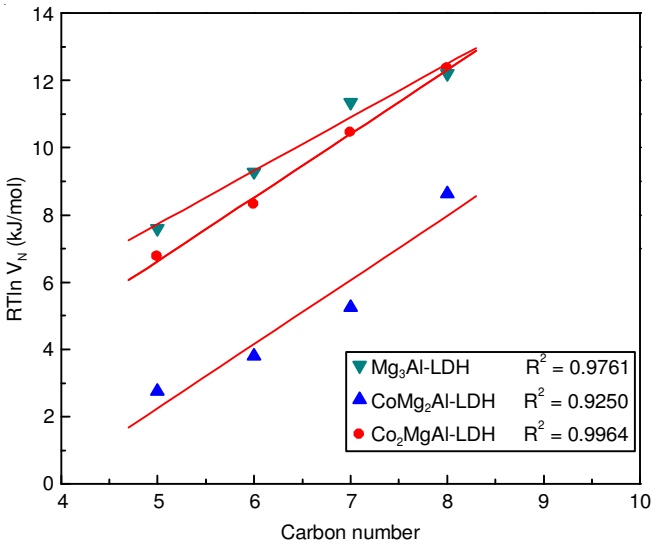

Fig. 2. Plot of RTln V_N values *versus* carbon number for $Co_xMg_{3-x}Al$-LDHs (x = 0-2) to determine γ_s^D

TABLE-2
γ_s^D VALUES OF $Ni_xMg_{3-x}Al$-LDHs AND $Co_xMg_{3-x}Al$-LDHs (x = 0-3)

LDHs	Mg_3Al	Mg_2NiAl	$MgNi_2Al$	Ni_3Al
γ_s^D (mJ m^{-2})	48.02	36.49	26.31	13.58
LDHs	Mg_3Al	Mg_2CoAl	$MgCo_2Al$	Co_3Al
γ_s^D (mJ m^{-2})	48.02	53.77	52.65	66.24

$Ni_xMg_{3-x}Al$-LDHs, γ_s^D showed a decreasing trend and the surface activity decreased, while the stability generally enhanced. On the other side, with the increasing of Co^{2+} in $Co_xMg_{3-x}Al$-LDHs, γ_s^D showed a increasing trend, the surface activity increased, while the stability reduced.

This phenomenon was presumably due to the reason that Mg^{2+} was generally replaced by Co^{2+} through isomorphous substitution to form Co-O_2 octahedron, which increased the distortion degree of the system, leading the hydrogen bonding and electrostatic force between the subject and object decrease gradually, and the absolute value of the binding energy decreased, so the system stability decreased.

Analyzing the dispersive component of surface energy between $Ni_xMg_{3-x}Al$-LDHs and $Co_xMg_{3-x}Al$-LDHs, it is found that the former were smaller. This may be due to the substitution of Ni^{2+}, the electron was transferred from the layer to the guest anion, which led to the enhancement of supramolecular interaction and the binding energy of the system, resulted in $Ni_xMg_{3-x}Al$-LDHs appear more stable. The above conclusions were consistent with the results of relevant literature [13] and theoretical results.

XRD analysis: As shown in Fig. 3, the crystal sharp of the hydrotalcites were relatively single and the characteristic diffraction peaks were close to each other, judging that the layer spacing was similar. The ionic radius of Ni^{2+} and Co^{2+} are 0.0690 nm and 0.0745 nm, respectively which are similar to Mg^{2+} (0.0720 nm), having little effect on the structure of hydrotalcite, but still presented certain regularity. Compared with Ni^{2+} and Co^{2+} samples' layer spacing, it is found that with the increasing of the incoming element on the plate, layer spacing changed slightly. In $Co_xMg_{3-x}Al$-LDHs system, with more and more Co^{2+} supersede Mg^{2+} by isomorphous substitution, layer spacing decreased to a certain extent, one each for 0.7887 nm, 0.7813 nm and 0.7708 nm. While spacing changes in $Ni_xMg_{3-x}Al$-LDHs showed the similar trends, which was consistent with the trend of lattice constants a and c.

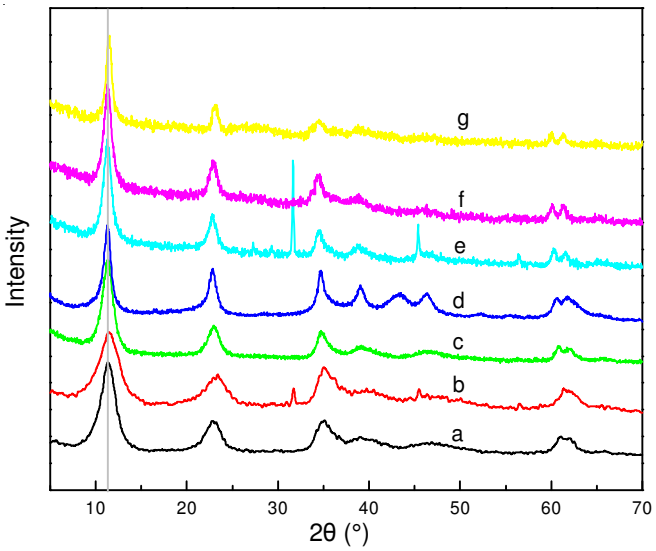

Fig. 3. XRD patterns of a-Ni_3Al-LDHs, b-$MgNi_2Al$-LDHs, c-Mg_2NiAl-LDHs, d-Mg_3Al-LDHs, e-Mg_2CoAl-LDHs, f-$MgCo_2Al$-LDHs, g-Co_3Al-LDHs

The theoretical simulation results showed that with the introduction of Ni^{2+}, the valence electron configuration of metal ions changed, while the plate structure did not cause serious distortion and each M-O bond length decreased gradually. The average bond length gradually reduced from 0.2045 nm (Mg_3Al-LDHs) to 0.1986 nm ($Ni_xMg_{3-x}Al$-LDHs). According to crystal field theory, the interaction between the central ion and ligand was called electrostatic effect, for the valence electron of the central metal atom passed out, led to the decreasing of the electron repulsion between the central ion and ligand. Therefore, the coordination bond would be stronger, resulting in a more stable octahedron, so the metal ion distance between the plate reduced gradually. The same theoretical simulation method was also suitable for $Co_xMg_{3-x}Al$-LDHs, the conclusion

of the two systems were consistent with the results obtained from the IGC test.

FT-IR analysis: The FTIR spectra of seven samples at absorption peak of 3496-3443 cm $^{-1}$ are shown in Fig. 4. They were mainly composed by the stretching vibrations between the layer board hydroxyl and interlayer water molecules, compared with hydroxyl free radical (3600 cm^{-1}), the peaks moved to low wavenumber, indicating that strong hydrogen bonding existed between interlayer water and layer board hydroxyl or carbonate. The vibration peaks of Fig. 4 are listed in Table-3.

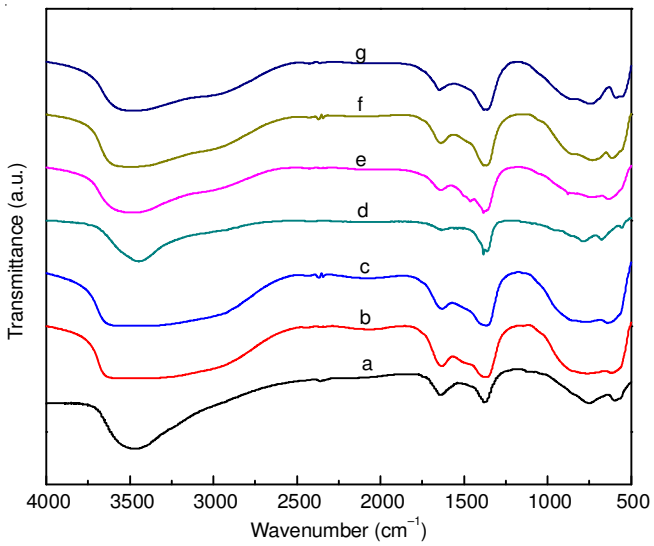

Fig. 4. FTIR spectra of a-Ni_3Al-LDHs, b-$MgNi_2Al$-LDHs, c-Mg_2NiAl-LDHs, d-Mg_3Al-LDHs, e-Mg_2CoAl-LDHs, f-$MgCo_2Al$-LDHs, g-Co_3Al-LDHs

TABLE-3
FTIR DATA OF $Ni_xMg_{3-x}Al$-LDHs AND $Co_xMg_{3-x}Al$-LDHs (x = 0-3)

System	a	b	c	d
Ni_3Al-LDHs	3478	1640	1380	415
$MgNi_2Al$-LDHs	3485	1633	1367	422
Mg_2NiAl-LDHs	3478	1631	1367	436
Mg_3Al-LDHs	3451	1629	1382	441
Mg_2CoAl-LDHs	3489	1636	1373	422
$MgCo_2Al$-LDHs	3496	1642	1373	428
Co_3Al-LDHs	3481	1650	1373	436

a. Stretching vibrations between layer board hydroxyl and interlayer water, b. H_2O bending vibration, c. CO_3^{2-} Symmetric vibration, d. M-O-M vibration.

As a certain amount of water inserted into the surface adsorbed water and interlayer space of hydrotalcite, a bending vibration peak of crystalline water rise in 1650-1629 cm^{-1} region Compared the vibration of interlayer CO_3^{2-} position at 1382-1367 cm^{-1} with the free state CO_3^{2-} (1430 cm^{-1}), the former moved to low wave number, demonstrating that hydrogen bonding existed in interlayer CO_3^{2-} and interlayer water molecules. With the increasing of Ni^{2+} and Co^{2+}, interlayer CO_3^{2-} remains substantially unchanged, meaning that the chemical environment in which it existed still unchanged significantly.

Combining the FTIR data (Table-3) and Mulliken bond population analysis (Table-4), it is found that with increase of Ni^{2+} in $Ni_xMg_{3-x}Al$-LDHs, metal oxygen bond vibration peak moved to low wave number slightly. It was due to the increasing of Ni^{2+} in $Ni_xMg_{3-x}Al$-LDHs changed the M-O bond in laminate

TABLE-4
MULLIKEN BOND POPULATION (e) OF $Ni_nMg_{3-n}Al$-LDHs (n=0-3)

System	Al-O	Mg-O	Ni-O	H-O
I	0.398	-0.723	–	0.575
II	0.370	-0.784	0.275	0.570
III	0.351	-0.857	0.242	0.578
IV	0.318	–	0.203	0.575

from covalent to ionic gradually, indicating the covalent bonds decreased in the isomorphous substitution process, while the ionic bonds increased. Thus, the whole system changed from the covalent crystals to the ionic crystal gradually and electrostatic interaction increase.

Combined the data in Table-3 and Table-5, with increasing Co^{2+} in $Co_xMg_{3-x}Al$-LDHs, metal oxygen bond vibration peak moved to high wavenumber slightly, because the theoretical charge population of Al was 1.370-1.660 e, while Mg was 1.680-2.010 e and Co was 0.586-0.860 e. It was evident that the electrostatic force between metal cations and other anions was in order of $Mg^{2+} > Al^{3+} > Co^{2+}$. Thus, the energy of sample decreased with the increasing Co^{2+}, and finally moved to high wavenumber.

TABLE-5
MULLIKEN ATOMIC POPULATION (e)
OF $Co_nMg_{3-n}Al$-LDHs (n = 0-3)

System	Al	Mg	Co	Layer
I	1.420	1.668	–	0.64
II	1.510	1.810	0.586	0.67
III	1.580	1.970	0.705	0.69
IV	1.700	–	0.860	0.72

Conclusion

In summary, $Ni_xMg_{3-x}Al$-LDHs and $Co_xMg_{3-x}Al$-LDHs (x = 0-3) with catalytic activity were synthesized through a co-precipitation method. All the hydrotalcites were characterized by inverse gas chromatography, X-ray diffraction and FT-IR. It is found that with the increase of Ni^{2+} in $Ni_xMg_{3-x}Al$-LDHs, the surface free energy decreased and the stability increased, which were consistent with the computer simulated results. While, with the increase of Co^{2+}, the surface energy dispersive component increased and the stability decreased. The adsorption capacity of $Co_xMg_{3-x}Al$-LDHs were larger than $Ni_xMg_{3-x}Al$-LDHs if the x were equal. The γ_s^D values of $Co_xMg_{3-x}Al$-LDHs were larger than $Ni_xMg_{3-x}Al$-LDHs, indicating that LDHs with Co^{2+} possess more powerful surface activities and LDHs with Ni^{2+} showed higher stability than $Co_xMg_{3-x}Al$-LDHs and Mg_3Al-LDHs.

ACKNOWLEDGEMENTS

The authors thank The Public Welfare Analysis of Science and Technology Plan Projects of Zhejiang Province of China (2015C37034).

REFERENCES

1. S. Kannan, *Catal. Surv. Asia*, **10**, 117 (2006); https://doi.org/10.1007/s10563-006-9012-y.
2. A. Tsujimura, M. Uchida and A. Okuwaki, *J. Hazard. Mater.*, **143**, 582 (2007); https://doi.org/10.1016/j.jhazmat.2006.09.073.

3. A. Vallet, M. Besson, G. Ovejero and J. García, *J. Hazard. Mater.*, **227-228**, 410 (2012); https://doi.org/10.1016/j.jhazmat.2012.05.081.
4. M. Munoz, S. Moreno and R. Molina, *Int. J. Hydrogen*, **37**, 18827 (2012); https://doi.org/10.1016/j.ijhydene.2012.09.132.
5. Y. Zhao, Q.-Z. Jiao, J. Liang and C.-H. Li, *Chem. Res. Chin. Univ.*, **21**, 471 (2005).
6. B.-H. Liu, H.-L. Zhang and J.-Y. Shen, *Chin. J. Inorg. Chem.*, **21**, 43 (2005).
7. Nai-Qiu Zhao, Master Dissertation, Beijing University of Chemical Technology, Beijing, China (2008).
8. G.S. Dritsas, K. Karatasos and C. Panayiotou, *J. Chromatogr. A*, **1216**, 8979 (2009); https://doi.org/10.1016/j.chroma.2009.10.050.
9. N. El-Thaher and P. Choi, *Ind. Eng. Chem. Res.*, **51**, 7022 (2012); https://doi.org/10.1021/ie202739x.
10. J.M. Chen and N. Yan, *BioResources*, **7**, 4132 (2012).
11. F. Zhang, X.-X. Cao, Z.-M. Ni and F.-F. Xing, *Chin. J. Inorg. Chem.*, **25**, 271 (2009).
12. X. Fu, Z. Ni and J. Liu, *Acta Chim. Sin.*, **70**, 968 (2012); https://doi.org/10.6023/A1112291.
13. N. Zhe-Ming, L. Yuan and S. Wei, *Chin. J. Inorg. Chem.*, **28**, 2051 (2012).
14. S.K. Yun and T. Pinnavaia, *J. Chem. Mater.*, **7**, 348 (1995); https://doi.org/10.1021/cm00050a017.
15. M. Ruckriem, A. Inayat, D. Enke, R. Gläser, W.-D. Einicke and R. Rockmann, *Colloid Surf. A*, **357**, 21 (2010); https://doi.org/10.1016/j.colsurfa.2009.12.001.
16. A. Askin and D. Topaloglu Yazici, *Chromatographia*, **61**, 625 (2005); https://doi.org/10.1365/s10337-005-0558-z.
17. A. Voelkel, B. Strzemiecka, K. Adamska and K. Milczewska, *J. Chromatogr. A*, **1216**, 1551 (2009); https://doi.org/10.1016/j.chroma.2008.10.096.